



Since January 2020 Elsevier has created a COVID-19 resource centre with free information in English and Mandarin on the novel coronavirus COVID-19. The COVID-19 resource centre is hosted on Elsevier Connect, the company's public news and information website.

Elsevier hereby grants permission to make all its COVID-19-related research that is available on the COVID-19 resource centre - including this research content - immediately available in PubMed Central and other publicly funded repositories, such as the WHO COVID database with rights for unrestricted research re-use and analyses in any form or by any means with acknowledgement of the original source. These permissions are granted for free by Elsevier for as long as the COVID-19 resource centre remains active.

SD-OCT assessment of macular and optic nerve alterations in patients recovered from COVID-19



Aysegul Mavi Yildiz, MD, FEBO, FICO, MRCSEd,* Gamze Ucan Gunduz, MD,[†] Ozgur Yalcinbayir, MD,*[†] Nilufer Aylin Acet Ozturk, MD,[‡] Remzi Avci, MD,* Funda Coskun[‡]

Objective: To quantify microstructural alterations in the macula and peripapillary retinal nerve fibre layer (RNFL) in patients recovered from coronavirus disease 2019 (COVID-19) using spectral domain optical coherence tomography (SD-OCT).

Design: Retrospective, observational.

Participants: This comparative, cross-sectional study included patients who recovered from COVID-19 (Group 1) and age- and sex-matched normal controls (Group 2).

Methods: A comprehensive ophthalmic examination, including best-corrected visual acuity and biomicroscopic anterior and posterior segment examination was performed. SD-OCT analysis of the macula and peripapillary RNFL was obtained for each participant. In addition, patient demographics and comorbidities were recorded.

Results: 238 eyes of 122 subjects (Group 1: n = 63; Group 2: n = 59) were included. The incidence of coexisting comorbidity was higher in Group 1 (n = 26/63, 41.3%) compared with Group 2 (n = 12/59, 20.3%) ($p = 0.013$). The central foveal thickness (CFT) was significantly higher in Group 1 ($271.0 \pm 26.8 \mu\text{m}$) than Group 2 ($263.2 \pm 22.0 \mu\text{m}$) ($p = 0.015$). The average outer nuclear layer (ONL) thickness at central fovea in Group 1 ($85.4 \pm 13.3 \mu\text{m}$) was significantly thicker than that in Group 2 ($81.4 \pm 15.2 \mu\text{m}$) ($p = 0.035$). The mean peripapillary RNFL thickness of Group 1 ($102.6 \pm 8.8 \mu\text{m}$) and Group 2 ($100.9 \pm 8.3 \mu\text{m}$) were similar ($p = 0.145$). The mean choroidal thickness of groups at the fovea and at 1500 μm nasal and temporal to the fovea were not significantly different ($p > 0.05$ for all).

Conclusion: Significant thickness alterations in individual retinal layers and CFT was detected in post-COVID-19 patients. The increase in CFT and ONL thickness might be attributed to direct infection or viral-induced inflammatory response of retina.

Objectif: Quantifier les modifications microstructurales apparaissant dans la macula et la couche de fibres nerveuses rétinienne péripapillaires chez des patients qui ont subi une infection à coronavirus 2019 (COVID-19) grâce à la tomographie par cohérence optique en domaine spectral (SD-OCT, pour *spectral domain optical coherence tomography*).

Nature: Étude rétrospective d'observation.

Participants: Cette étude transversale comparative a porté sur des patients qui ont eu la COVID-19 (groupe 1) et sur des sujets sains appariés pour l'âge et le sexe (groupe 2).

Méthodes: On a procédé à un examen ophtalmologique complet – meilleure acuité visuelle corrigée et examen biomicroscopique des segments antérieur et postérieur – et à une analyse SD-OCT de la macula et de la couche de fibres nerveuses rétinienne péripapillaires de chaque participant. On a également noté leurs caractéristiques démographiques et leurs comorbidités.

Résultats: Ont ainsi été inclus 238 yeux de 122 sujets (groupe 1 : n = 63; groupe 2 : n = 59). L'incidence de comorbidités était plus élevée dans le groupe 1 (n = 26/63; 41,3 %) que dans le groupe 2 (n = 12/59; 20,3 %; $p = 0,013$). L'épaisseur centrale de la fovéa était significativement plus élevée dans le groupe 1 ($271,0 \pm 26,8 \mu\text{m}$) que dans le groupe 2 ($263,2 \pm 22,0 \mu\text{m}$; $p = 0,015$). L'épaisseur moyenne de la couche nucléaire externe dans la zone centrale de la fovéa des sujets du groupe 1 ($85,4 \pm 13,3 \mu\text{m}$) était significativement plus élevée que celle des sujets du groupe 2 ($81,4 \pm 15,2 \mu\text{m}$; $p = 0,035$). L'épaisseur moyenne de la couche de fibres nerveuses rétinienne péripapillaires était semblable dans les 2 groupes (groupe 1 : $102,6 \pm 8,8 \mu\text{m}$; groupe 2 : $100,9 \pm 8,3 \mu\text{m}$; $p = 0,145$). Enfin, l'épaisseur moyenne de la choroïde dans la fovéa, à 1500 μm en nasal de la fovéa et à 1500 μm en temporal de la fovéa ne différait pas significativement entre les 2 groupes ($p > 0,05$ pour l'ensemble des mesures).

Conclusion: On note des modifications significatives de l'épaisseur des couches rétinienne individuelles et de l'épaisseur centrale de la fovéa chez des patients qui ont eu la COVID-19. Cette augmentation de l'épaisseur centrale de la fovéa et de la couche nucléaire externe peut tenir à l'infection elle-même ou à une réponse inflammatoire virale dans la rétine.

Since the coronavirus disease 2019 (COVID-19) caused by the severe acute respiratory syndrome coronavirus 2 (SARS-CoV-2) emerged from China in December 2019, a large number of studies have been published from around the world. Although, the classical presentation of COVID-19 includes fever and respiratory tract symptoms, a wide spectrum of clinical manifestations, including cardiovascular,¹ neurological,² gastrointestinal,³ hematological,⁴ dermatological,⁵ and ocular⁶ involvement, have been reported.

SARS-CoV-2 enters host cells via the angiotensin-converting enzyme 2 (ACE2) receptor, which is expressed in various tissues, including the vascular endothelium and neurosensory retina.^{7,8} Increased rates of both the arterial and venous thromboembolism have been reported in patients with COVID-19, which could be attributed to direct viral invasion and inflammation of the endothelial cells.⁹ Accordingly, ischemic retinal changes—including flame-shaped hemorrhages, cotton wool spots, and retinal sectorial pallor—have been reported in patients who recovered from SARS-CoV-2 infection.^{10,11} A recent publication on retinal microvascular manifestations of SARS-CoV-2 infection indicated that the mean macular capillary vessel density was significantly lower in the COVID group compared with age-matched normal controls.¹² Accordingly, significantly lower levels of peripapillary perfusion density were detected in post-COVID-19 patients in another recent study.¹³

On the other hand, central nervous system (CNS) involvement in the course of COVID-19 and neurotropic potential of SARS-CoV-2 have been reported in the literature.¹⁴ Moreover, in a recent study, viral ribonucleic acid (RNA) of SARS-CoV-2 has been detected in retinas of deceased patients with COVID-19.¹⁵

Regarding the neuroinvasive and prothrombotic capabilities of SARS-CoV-2, it is likely to observe retinal manifestations in COVID-19. Therefore, the aim of our study was to identify microstructural changes in the macula and the peripapillary retinal nerve fibre layer (RNFL) in post-COVID-19 patients.

Methods

Design

This cross-sectional study was conducted between April 2020 and October 2020. The study was approved by the Ethics Committee of Uludağ University Faculty of Medicine, Bursa, Turkey (July 14, 2020) before the study period. The research was conducted in accordance with the tenets of the Declaration of Helsinki. Written informed consent was obtained from all participants, consistent with Turkish National Research Ethics Committee resolution for research conducted during the COVID-19 pandemic.

Participants

A total of 63 patients with confirmed SARS-CoV-2 infection (Group 1) were included in this study. The diagnosis of COVID-19 was confirmed by a positive test result with real-

time, reverse transcription-polymerase chain reaction of a nasopharyngeal swab sample. The period between the date of the positive real-time, reverse transcription-polymerase chain reaction test result and ophthalmological examination ranged from 2 weeks to 8 weeks in the study group. The control group consisted of 59 age and sex-matched normal controls who consented to participate in the study.

Patients with diabetic retinopathy or any other choroidal/retinal pathologies, high myopia (an axial length ≥ 26.5 mm), uveitis, glaucoma, previous optic neuropathy, or history of any intraocular surgery or laser treatment (except for phacoemulsification) and pregnant or breastfeeding women were excluded. Participants in the control group were interviewed for potential signs and symptoms of COVID-19 and potentially exposed contacts. Individuals with a history of fever, dry cough, extreme fatigue, loss of taste or smell, severe headache, severe chest pain, sore throat, diarrhea, nausea and vomiting, conjunctivitis, nasal congestion/stuffy or runny nose, or new rash on skin and those with a history of close contact to a patient with confirmed COVID-19 within the last 2 weeks were excluded. Demographic characteristics, baseline comorbidities, and clinical data were recorded.

Ocular Parameters and Optical Coherence Tomography Imaging

All the participants underwent a complete ophthalmic examination, including manifest refraction, axial length measurement, best corrected visual acuity (BCVA), slit-lamp biomicroscopy, and dilated funduscopy. The BCVAs in Snellen values were converted to the logMAR. The manifest refraction was measured using an automatic refractometer (RF10, Canon Inc., Tokyo, Japan). The spherical equivalent (SE) refractive error was calculated by adding the sum of the sphere power with half of the cylinder power. The axial length was measured using Lenstar LS 900 (version 2.1.1, Haag-Streit AG, Koeniz, Switzerland).

The spectral domain optical coherence tomography (SD-OCT) examination was performed with the Spectralis (HRA + OCT, Heidelberg Engineering, Germany). The macular and peripapillary RNFL scans were obtained from all participants. Only well-centered images with a quality index of >15 were used for analysis. Images with artifacts were excluded.

The scanning of the macula was performed routinely by the fast macular cube scan, high-resolution 6 macular radial scans, and 25 raster lines spaced 200 μm apart. To center on the patient's fovea, real-time eye-tracking software (TruTrack, Heidelberg Engineering, Heidelberg, Germany) was used. The central foveal thickness, which was defined as the average of all points within the central 1 mm diameter circle surrounding fixation was recorded. In addition, the thicknesses of seven retinal layers defined by the Early Treatment Diabetic Retinopathy Study were automatically analyzed with the spectral domain optical coherence tomography (SD-OCT) device software (Segmentation Technology, Heidelberg Engineering GmbH, Heidelberg, Germany). The single layers measured were RNFL,

ganglion cell layer (GCL), inner plexiform layer (IPL), inner nuclear layer (INL), outer plexiform layer (OPL), outer nuclear layer (ONL), and retinal pigmented epithelium (RPE). In addition, the integrity of the RPE layer was assessed qualitatively and defined as irregular if it appeared blurred or interrupted on SD-OCT imaging.

The peripapillary RNFL thickness measurements were obtained with the SD-OCT using a circular scan pattern (diameter of 3.5 mm, 768A-scans); an online tracking system was used to compensate for eye movement. The RNFL thickness (from the inner margin of the internal limiting membrane to the outer margin of the RNFL layer) was automatically segmented using the Spectralis software (version 5.3.3.0). The global RNFL thickness and average RNFL thicknesses of superior [S], inferior [I], nasal [N], temporal [T], superior-temporal, superior-nasal, inferior-nasal and inferior-temporal quadrants were recorded.

The choroidal thickness (CT) measurements were performed at the fovea and at 1500 μm nasal and temporal to the center of the fovea using enhanced depth imaging SD-OCT (Spectralis, Heidelberg Engineering, Heidelberg, Germany) and Heidelberg Eye Explorer software (version 1.9.10.0). The thickness measurement was obtained manually using the caliper function of the device from the outer portion of the RPE to the inner surface of the sclera.

Statistical Analysis

The data were examined by the Shapiro Wilk test to determine whether or not it presents normal distribution. The results were presented as mean \pm standard deviation or frequency and percentage. Normally distributed data were compared with independent samples *t* test or one-way analysis of variance. Kruskal-Wallis and Mann-Whitney U tests were used for nonnormally distributed data. Bonferroni test was used as multiple comparison test. Categorical variables were compared using Pearson χ^2 test, Fisher exact test, and

Fisher-Freeman-Halton test. A *p* value <0.05 was considered significant. Statistical analyses were performed with IBM SPSS version 23.0 (IBM Corp. Released 2015. IBM SPSS Statistics for Windows, Version 23.0. Armonk, NY: IBM Corp.).

Results

A total of 236 eyes of 122 participants were included in this study. Group 1 consisted of 119 eyes of 62 patients who had a confirmed diagnosis of COVID-19, whereas Group 2 consisted of 117 eyes of 59 normal controls. Eight eyes were excluded owing to central corneal scar secondary to previous ocular trauma ($n = 2/8$), mature cataract ($n = 1/8$), and signal strength score less than 20 db ($n = 5/8$). Thirty (47%) of the patients in Group 1 were hospitalized for COVID-19. However, none of these patients required endotracheal intubation at any time during hospitalization. All participants were asymptomatic at the time of examination.

The mean age of the subjects in Group 1 and Group 2 was 44.6 ± 12.6 years and 43.5 ± 12.1 years respectively. No statistically significant difference was detected between groups with regard to age ($p = 0.608$), sex ($p = 0.225$), BCVA ($p = 0.054$), lens status ($p = 0.498$), SE ($p = 0.595$), and axial length ($p = 0.304$). However, in subgroup analysis, the mean age of the patients with COVID-19 who were hospitalized (50.1 ± 14.1 years) was significantly higher than that of the patients with COVID-19 who were not hospitalized (39.7 ± 8.8 years, $p = 0.003$). All participants had a Early Treatment Diabetic Retinopathy Study chart BCVA value greater than 20/25. Preoperative demographic characteristics of patients are summarized in Table 1.

The incidence of comorbidity was significantly higher in the study group ($n = 26/62$, 41.3%) compared with the control group ($n = 12/59$, 20.3%) ($p = 0.013$) (Table 1). Moreover, subgroup analysis revealed that the incidence of

Table 1—Ophthalmologic features and demographic characteristics of subjects in Group 1 (COVID-19 Group) and Group 2 (control group)

	Group 1 (n = 63,119 eyes)	Group 2 (n = 59, 117 eyes)	<i>p</i>
Age (years)	44.6 \pm 12.6 (22–82)	43.5 \pm 12.1 (22–69)	0.608*
Sex (Female/Male)	36/27	40/19	0.225 [†]
Comorbidity (%)	26 (41.3%)	12 (20.3%)	0.013
1. COPD	7 (11.1%)	1 (1.6%)	
2. Diabetes mellitus	10 (15.8%)	5 (8.4%)	
3. Hypertension	13 (20.6%)	7 (11.8%)	
4. Chronic renal insufficiency	2 (3.1%)	0 (0%)	
5. Hypothyroidism	3 (4.7%)	1 (1.6%)	
6. Coronary artery disease	3 (4.7%)	1 (1.6%)	
7. Malignant neoplasm	0 (0%)	1 (1.6%)	
8. Mood disorder	3 (4.7%)	1 (1.6%)	
9. Behçet disease	1 (1.5%)	0 (0%)	
BCVA (Snellen)	0.99 \pm 0.05 (0.80–1.00)	0.97 \pm 0.10 (0.50–1.00)	0.054*
Lens status: phakic/pseudophakic	117/2	117/0	0.498
Axial length (mm)	23.46 \pm 0.85	23.58 \pm 0.89	0.304*
Spherical Equivalent (D)	0.02 \pm 0.55	0.06 \pm 0.23	0.595*

BCVA, best corrected visual acuity; COPD, chronic obstructive pulmonary disease; D, diopters.

Descriptive statistics were given as mean \pm standard deviation (minimum–maximum) or frequency with percentage. A *p* value <0.05 was considered significant.

*Independent samples *t* test.

[†]Pearson χ^2 test.

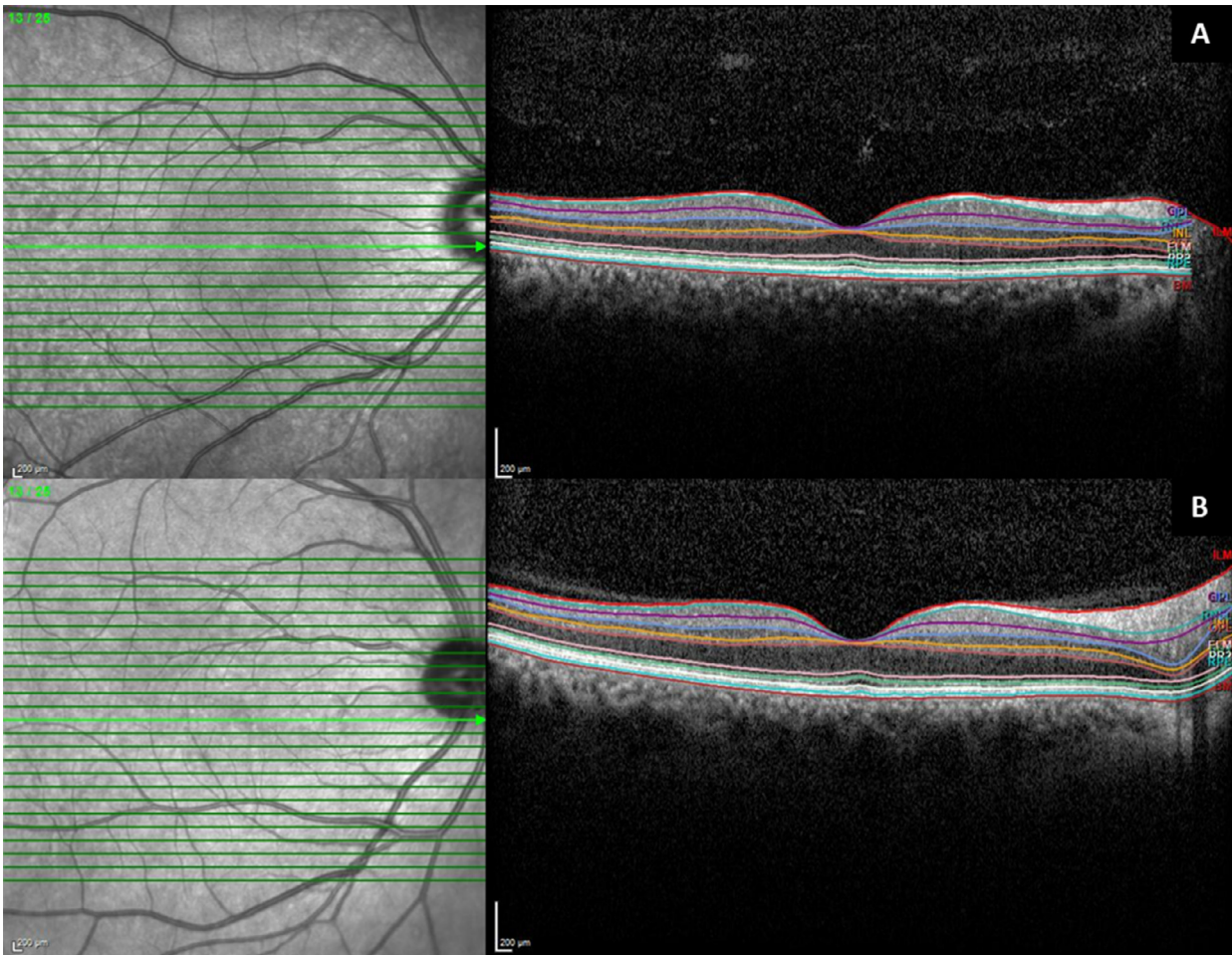


Fig. 1—Spectral domain optical coherence tomography (SD-OCT) images of the macula of a normal control (A) versus a patient who recovered from COVID-19 (B). Note the remarkable enlargement of the outer nuclear layer in the segmented view of the post-COVID-19 case.

comorbidities was significantly higher in patients with COVID-19 who were hospitalized ($n = 19/30$) compared with the patients with COVID-19 patients who were not hospitalized ($n = 7/33$, $p < 0.01$). In addition, 12 of the patients in Group 1 and 5 of the patients in Group 2 had more than 1 coexisting systemic disease. The most common comorbidities were chronic obstructive pulmonary disease (COPD), hypertension, and diabetes mellitus.

The major ocular complaints during the acute phase of COVID-19 disease included transient blurring of vision ($n = 2/62$), watery discharge ($n = 2/62$), pain and light sensitivity ($n = 2/62$), and itchy eyes ($n = 1/62$). However, none of the patients showed signs of keratitis, conjunctivitis, or uveitis on slit lamp-examination.

The mean central foveal thickness (CFT) in Group 1 ($271.0 \pm 26.8 \mu\text{m}$) was significantly higher than that of Group 2 ($263.2 \pm 22.0 \mu\text{m}$, $p = 0.015$). Similarly, the mean ONL thickness was higher in Group 1 ($85.4 \pm 13.3 \mu\text{m}$) compared with Group 2 ($81.4 \pm 15.2 \mu\text{m}$, $p = 0.035$) (Figure 1). Furthermore, in subgroup analysis, the mean thickness of the ONL in the patients with COVID-19 who were hospitalized ($89.0 \pm 13.6 \mu\text{m}$) was significantly higher

than that of patients with COVID-19 who were not hospitalized ($82.1 \pm 12.3 \mu\text{m}$, $p = 0.003$). However, mean thicknesses of the NFL, GCL, IPL, INL, OPL, and RPE in Group 1 and Group 2 were similar ($p > 0.05$ for all) (Table 2). In addition, focal irregularity of the RPE layer was detected in 14.9% of the participants in Group 1 and 10.4% of the participants in Group 2 ($p = 0.309$).

The mean subfoveal CTs of Group 1 and Group 2 were $341.6 \pm 79.7 \mu\text{m}$ and $340.7 \pm 86.2 \mu\text{m}$ respectively ($p = 0.936$). The mean CTs at 1500 μm nasal to the fovea in Group 1 and Group 2 were $273 \pm 79.4 \mu\text{m}$ and $272.9 \pm 80.6 \mu\text{m}$ respectively ($p = 0.956$). Corresponding values for CTs at 1500 μm temporal to the fovea were $283.9 \pm 77.9 \mu\text{m}$ and $284.2 \pm 73.3 \mu\text{m}$ respectively ($p = 0.974$).

The global mean peripapillary RNFL thicknesses in Group 1 ($102.6 \pm 8.8 \mu\text{m}$) and Group 2 ($100.9 \pm 8.3 \mu\text{m}$) were similar ($p = 0.145$). However, the RNFL thickness in the superior (Group 1: $130.0 \pm 33.2 \mu\text{m}$; Group 2: $119.7 \pm 35.4 \mu\text{m}$) and inferotemporal quadrants (Group 1: $98.0 \pm 20.4 \mu\text{m}$; Group 2: $104.8 \pm 24.1 \mu\text{m}$) were different between groups ($p = 0.017$ and $p = 0.021$ respectively) (Table 3).

Table 2—Comparison of foveal and choroidal thicknesses of subjects in Group 1 (COVID-19 group) and Group 2 (control group) using spectral domain optical coherence tomography. Choroidal thickness is measured by enhanced depth imaging optical coherence tomography subfoveally, 1500 μm nasal and 1500 μm temporal to the fovea.

	Group 1 (n = 119 eyes)	Group 2 (n = 117 eyes)	<i>p</i>
CFT (μm)	271.0 \pm 26.8	263.2 \pm 22.0	0.015
NFL thickness (μm)	13.0 \pm 5.5	12.0 \pm 3.8	0.115*
GCL thickness (μm)	17.5 \pm 11.0	15.5 \pm 6.2	0.091 [†]
IPL thickness (μm)	21.3 \pm 6.7	19.9 \pm 4.8	0.065 [‡]
INL thickness (μm)	21.5 \pm 7.8	22.2 \pm 7.2	0.513 [‡]
OPL thickness (μm)	26.4 \pm 7.8	27.0 \pm 7.3	0.490 [‡]
ONL thickness (μm)	85.4 \pm 13.3	81.4 \pm 15.2	0.035*
RPE thickness (μm)	15.7 \pm 2.0	15.2 \pm 2.7	0.089 [‡]
Subfoveal disruption of the RPE layer	18 (14.9%)	12 (10.4%)	0.309 [‡]
Subfoveal choroidal thickness (μm)	341.6 \pm 79.7	340.7 \pm 86.2	0.936
Choroidal thickness in nasal quadrant (μm)	273 \pm 79.4	272.9 \pm 80.6	0.956
Choroidal thickness in temporal quadrant (μm)	283.9 \pm 77.9	284.2 \pm 73.3	0.974

COVID-19, coronavirus disease 2019; CFT, central foveal thickness; NFL, nerve fibre layer; GCL, ganglion cell layer; IPL, inner plexiform layer; INL, inner plexiform layer; OPL, outer plexiform layer; ONL, outer nuclear layer; RPE, retinal pigment epithelium.

Descriptive statistics were given as mean \pm standard deviation or frequency with percentage. A *p* value < 0.05 was considered significant.

*Independent samples *t* test.

[†]Pearson χ^2 test.

[‡]Mann–Whitney *U*.

Table 3—Comparison of peripapillary retinal nerve fibre layer thickness (μm) in different quadrants of subjects in Group 1 (COVID-19 group) and Group 2 (control group) using spectral domain optical coherence tomography

	Group 1 (n = 119 eyes)	Group 2 (n = 117 eyes)	<i>p</i>
Whole (μm)	102.6 \pm 8.8	100.9 \pm 8.3	0.145*
Superior quadrant (μm)	130.0 \pm 33.2	119.7 \pm 35.4	0.017*
Inferior quadrant (μm)	146.5 \pm 35.8	142.7 \pm 25.6	0.321*
Nasal quadrant (μm)	61.1 \pm 16.3	60.3 \pm 16.8	0.706*
Temporal quadrant (μm)	56.2 \pm 10.1	56.1 \pm 10.0	0.920*
Superonasal quadrant (μm)	115.8 \pm 26.9	112.9 \pm 25.1	0.404*
Superotemporal quadrant (μm)	104.9 \pm 23.6	106.5 \pm 23.5	0.604*
Inferonasal quadrant (μm)	95.4 \pm 27.5	93.9 \pm 23.9	0.660*
Inferotemporal quadrant (μm)	98.0 \pm 20.4	104.8 \pm 24.1	0.021*

COVID-19, coronavirus disease 2019.

Descriptive statistics were given as mean \pm standard deviation. A *p* value < 0.05 was considered significant.

*Independent samples *t* test.

Given that study results might have been affected by the mix of potential confounders, including enrollment of both eyes and presence of comorbidities, we have also conducted a subgroup analysis. Participants with systemic diseases including diabetes and hypertension and/or visual acuity < 0.8 were excluded. Further statistical analysis involved only one eye (right) in each participant. Group 1 consisted of 45 patients, whereas Group 2 included 50 healthy controls. The BCVA in Group 1 and Group 2 were 1.0 ± 0.0 and 0.98 ± 0.04 respectively ($p = 0.097$). The mean CFT (Group 1: $272.3 \pm 26.4 \mu\text{m}$, Group 2: $262.0 \pm 21.3 \mu\text{m}$) and ONL thickness (Group 1: $86.7 \pm 12.2 \mu\text{m}$, Group 2: $80.5 \pm 13.3 \mu\text{m}$) was significantly thicker in the post-COVID group than in the control group ($p = 0.048$ and $p = 0.018$ respectively). However, mean thicknesses of the nerve fibre layer (NFL) ($p = 0.368$), GCL ($p = 0.329$), IPL ($p = 0.353$), INL ($p = 0.504$), OPL ($p = 0.641$), RPE ($p = 0.367$), and RNFL in all quadrants ($p > 0.05$ for all) were similar.

Discussion

In the current study, qualitative and quantitative assessment of the macula and peripapillary RNFL was performed using SD-OCT imaging. The data of post-COVID-19 patients was compared with age- and sex-matched normal controls to evaluate SARS-

CoV-2 related microstructural alterations. In the literature, reported cases of COVID-19 have a wide range of symptoms from mild complaints, such as fever and cough, to more critical cases associated with difficulty in breathing.¹⁶ It is estimated that about 17.9% of positive patients show no symptoms. Therefore, we interviewed the subjects in the control group for potential signs of COVID-19 and suspected individuals were excluded.

There was no significant difference between groups with regard to the BCVA, SE, and axial length. The thicknesses of the central macula (within 1 mm diameter) and ONL were significantly higher in post-COVID-19 patients compared with normal controls. However, there was no significant difference between the groups with regard to the thicknesses of other remaining retinal layers (NFL, GCL, IPL, INL, OPL, and RPE). Similarly, no significant difference was detected between the CT measurements at the fovea, at 1500 μm nasal to the fovea, and at 1500 μm temporal to the fovea of groups. In addition, subgroup analysis among patients in Group 1 revealed that the mean thickness of the ONL was significantly higher in the patients who were hospitalized compared with patients who were not hospitalized. Therefore, presence and severity of SARS-CoV-2 infection appears to be positively correlated with the outer retinal thickness alterations. Possible underlying mechanisms responsible for retinal involvement over the course of COVID-19 are discussed below.

Angiotensin-converting enzyme 2 (ACE2) is widely expressed throughout the body, including the respiratory system, cardiovascular system (endothelial cells, vascular smooth muscle cells), gut, kidneys, central nervous system, and retina, and has been identified as the cellular receptor of SARS-CoV-2, the causative virus of COVID-19.^{17,18} The existence of ACE2 receptors in the rod and cone layer has also been demonstrated in immunohistochemical studies on enucleated human eyes.¹⁹ Moreover, viral RNA of SARS-CoV-2 has been documented in retinal samples of patients with COVID-19.¹⁵ Experimental studies strongly suggest that ACE has vasodilatory, antiproliferative, and anti-inflammatory properties.²⁰ Accordingly, destruction of ACE2 receptors has been associated with multiorgan dysfunction owing to increased levels of reactive oxygen species, induction of fibrosis, hypertrophy, and inflammation. Therefore, decreased ACE2 expression in the neurosensory retinal cells and retinal vasculature could result in inflammation and oxidative stress, which are common factors involved in the pathogenesis of several retinal diseases.

On the other hand, systemic viral infections have been associated with interferon γ (IFN- γ)–mediated migration of microglial cells, which are mainly located in the inner retina and into the outer layers of the retina and subretinal space.²¹ Accumulation of microglia in the outer retina and the subretinal space is thought to be involved in the pathogenesis of chronic neurodegenerative diseases of the retina, such as age-related macular degeneration, diabetic retinopathy and retinal dystrophies.^{22–24} Accordingly, interferon-mediated immune response has shown to play a crucial role against SARS-CoV-2 infection.²⁵ Therefore, we hypothesize that the outer retinal thickening could also be a result of immune-mediated inflammation driven by retinal microglial cells.

Moreover, COVID-19 is associated with arterial and venous thrombotic complications, including myocardial infarction, ischemic stroke, and venous thromboembolism.²⁶ Recently, Marinho et al.¹⁰ reported a case series demonstrating retinal findings related with SARS-CoV-2 infection. All cases exhibited focal hyperreflective lesions at the level of ganglion cell and IPLs on SD-OCT. In addition, cotton wool spots and retinal microhemorrhages were detected in 4 out of 12 patients. However, Vavvas et al.²⁷ subsequently pointed out that these hyperreflective bands in the inner retina could possibly represent oblique sections and cross-sections of perifoveal normal retinal blood vessels. Accordingly, we did not observe any hyperreflective or hyporeflexive lesion in SD-OCT images of any subjects. Landecho et al.²⁸ concluded that 22% of the post-COVID-19 patients demonstrated cotton wool exudates on retinal examination. In contrast, we did not observe any ischemic retinal changes. A possible explanation is that ocular examination was conducted 2–8 weeks after diagnosis of COVID-19. Therefore, the cotton wool spots and flame hemorrhages might have disappeared within the first 2 weeks.

Abrishami et al.¹² conducted a study to assess microvascular changes in patients who recovered from COVID-19. The authors stated that the mean superficial and deep vascular densities in the foveal and parafoveal regions were significantly lower in the COVID cohort compared with the control group. In the current study we did not assess the retinal blood flow. Furthermore, the RNFL comparisons were not significantly different, especially with subgroup analysis to remove potential confounders.

We also analyzed the patient demographics in both groups. The number of patients with common comorbidities, including COPD, hypertension, diabetes, and coronary artery disease, were significantly higher in Group 1 compared with Group 2. Accordingly, Wang et al.²⁹ conducted a meta-analysis including 1558 patients with COVID-19. The authors concluded that hypertension, diabetes, COPD, cardiovascular disease, and cerebrovascular disease are major risk factors for patients with COVID-19. In addition, we conducted subgroup analysis among the post-COVID-19 cohort and found that the incidence of comorbidities and mean age were significantly higher in patients who were hospitalized compared with patients who were not hospitalized.

Limitations of our study include the cross-sectional design, lack of longitudinal observation of the patients, and lack of multimodal imaging, including simultaneous optical coherence tomography angiography and fundus fluorescein angiography. In addition, there may be many possible confounding factors that could influence the OCT parameters. First, including measurements from both eyes without adjusting for the correlated nature of the data may have had a substantial effect on the results. Second, presence of comorbidities, including diabetes and hypertension, might have influenced retinal thickness measurements. Strengths of this study include it being the largest group ever described in the literature of patients with retinal microstructural alterations possibly related to SARS-CoV-2. Furthermore, to the best of our knowledge, this is the first study evaluating the thicknesses of individual retinal layers of post-COVID-19 patients using SD-OCT.

In conclusion, our study demonstrated significant anatomical changes in individual retinal layers of post-COVID-19 patients for the first time. In light of the current literature, we suggest that thickening of ONL, which is comprised of the photoreceptor cell bodies, could be a marker of retinal inflammation. The possible mechanisms for retinal inflammation include direct neuronal invasion, IFN-mediated alterations in the retinal microenvironment during the course of systemic disease, or ischemia secondary to endophthalmitis. Alterations in the immune status of the retina during the course of COVID-19 might aggravate existing retinal diseases such as diabetic/ hypertensive retinopathy and age-related macular degeneration, where low-grade inflammation plays a role. Further studies with long-term follow up are needed to determine the definite consequences of COVID-19 related retinopathy.

References

- Zheng YY, Ma YT, Zhang JY, Xie X. COVID-19 and the cardiovascular system. *Nat Rev Cardiol* 2020 May;17:259–60.
- Niazkar HR, Zibae B, Nasimi A, Bahri N. The neurological manifestations of COVID-19: a review article. *Neurol Sci* 2020;41:1667–71.
- Gu J, Han B, Wang J. COVID-19: Gastrointestinal manifestations and potential fecal-oral transmission. *Gastroenterology* 2020;158:1518–9.
- Agbuduwe C, Basu S. Haematological manifestations of COVID-19: from cytopenia to coagulopathy. *Eur J Haematol* 2020;105:540–6.
- Fahmy DH, El-Amawy HS, El-Samongy MA, et al. COVID-19 and dermatology: a comprehensive guide for dermatologists. *J Eur Acad Dermatol Venereol*. 34:1388–94.
- Wu P, Duan F, Luo C, Liu Q, Qu X, Liang L, Wu K. Characteristics of ocular findings of patients with coronavirus disease 2019 (COVID-19) in Hubei province, China. *JAMA Ophthalmol* 2020;138:575–8.
- Bourgonje AR, Abdulle AE, Timens W, et al. Angiotensin-converting enzyme 2 (ACE2), SARS-CoV-2 and the pathophysiology of coronavirus disease 2019 (COVID-19). *J Pathol* 2020;251:228–48.
- Senanayake P, Drazba J, Shadrach K, et al. Angiotensin II and its receptor subtypes in the human retina. *Invest Ophthalmol Vis Sci* 2007;48:3301–11.
- Malas MB, Naazie IN, Elsayed N, Mathlouthi A, Marmor R, Clary B. Thromboembolism risk of COVID-19 is high and associated with a higher risk of mortality: a systematic review and meta-analysis. *EClinicalMedicine* 2020;29:100639.
- Marinho PM, Marcos AAA, Romano AC, Nascimento H, Belfort Jr. R. Retinal findings in patients with COVID-19. *Lancet* 2020;395:1610.
- Invernizzi A, Torre A, Parrulli S, et al. Retinal findings in patients with COVID-19: results from the SERPICO-19 study. *EClinicalMedicine* 2020;27:100550 Oct.
- Abrishami M, Emamverdian Z, Shoeibi N, et al. Optical coherence tomography angiography analysis of the retina in patients recovered from COVID-19: a case-control study. *Can J Ophthalmol* 2020;30813–9 S0008–4182.
- Savastano A, Crincoli E, Savastano MC, et al. Peripapillary retinal vascular involvement in early post-COVID-19 patients. *J Clin Med* 2020;9:2895.
- Conde Cardona G, Quintana Pájaro LD, Quintero Marzola ID, Ramos Villegas Y, Moscote Salazar LR. Neurotropism of SARS-CoV 2: mechanisms and manifestations. *J Neurol Sci* 2020;412:116824.
- Casagrande M, Fitzek A, Püschel K, et al. Detection of SARS-CoV-2 in human retinal biopsies of deceased COVID-19 patients. *Ocul Immunol Inflamm* 2020;28:721–5.
- Centers for Disease Control and Prevention (CDC). Coronavirus (COVID-19): symptoms of coronavirus. <https://www.cdc.gov/coronavirus/2019-ncov/symptoms-testing/symptoms.html>. Accessed April 18, 2020.
- Yan R, Zhang Y, Li Y, Xia L, Guo Y, Zhou Q. Structural basis for the recognition of SARS-CoV-2 by full-length human ACE2. *Science* 2020;367:1444–8.
- Rodrigues Prestes TR, Rocha NP, Miranda AS, Teixeira AL, Simoes-E-Silva AC. The anti-inflammatory potential of ACE2/angiotensin-(1-7)/Mas receptor axis: evidence from basic and clinical research. *Curr Drug Targets* 2017;18:1301–13.
- White AJ, Cheruvu SC, Sarris M, et al. Expression of classical components of the renin-angiotensin system in the human eye. *J Renin Angiotensin Aldosterone Syst* 2015;16:59–66.
- Gheblawi M, Wang K, Viveiros A, et al. Angiotensin-converting enzyme 2: SARS-CoV-2 receptor and regulator of the renin-angiotensin system: celebrating the 20th anniversary of the discovery of ACE2. *Circ Res* 2020;126:1456–74.
- Zinkernagel MS, Chinnery HR, Ong ML, et al. Interferon γ -dependent migration of microglial cells in the retina after systemic cytomegalovirus infection. *Am J Pathol* 2013;182:875–85.
- Combadiere C, Feumi C, Raoul W, et al. CX3CR1-dependent subretinal microglia cell accumulation is associated with cardinal features of age-related macular degeneration. *J Clin Invest* 2007;117:2920e2928.
- Omri S, Behar-Cohen F, de Kozak Y, et al. Microglia/macrophages migrate through retinal epithelium barrier by a transcellular route in diabetic retinopathy: role of PKCzeta in the Goto Kakizaki rat model. *Am J Pathol* 2011;179:942–53.
- Hughes EH, Schlichtenbrede FC, Murphy CC, et al. Generation of activated sialoadhesin-positive microglia during retinal degeneration. *Invest Ophthalmol Vis Sci* 2003;44:2229–34.
- Portela Sousa C, Brites C. Immune response in SARS-CoV-2 infection: the role of interferons type I and type III. *Braz J Infect Dis* 2020;24:428–33.
- Piazza G, Campia U, Hurwitz S, et al. Registry of arterial and venous thromboembolic complications in patients with COVID-19. *J Am Coll Cardiol* 2020;76:2060–72.
- Vavvas DG, Sarraf D, Sadda SR, et al. Concerns about the interpretation of OCT and fundus findings in COVID-19 patients in recent Lancet publication. *Eye (Lond)* 2020;34:2153–4.
- Landecheo MF, Yuste JR, Gándara E, et al. COVID-19 retinal microangiopathy as an in vivo biomarker of systemic vascular disease? *J Intern Med* 2020;289:116–20.
- Wang B, Li R, Lu Z, Huang Y. Does comorbidity increase the risk of patients with COVID-19: evidence from meta-analysis. *Aging (Albany NY)* 2020;12:6049–57 8.

Footnotes and Disclosure

The authors have no proprietary or commercial interest in any materials discussed in this article.

From the *Bursa Retina Eye Hospital, Department of Ophthalmology, Bursa, Turkey; †Bursa Uludag University School of Medicine, Department of Ophthalmology, Bursa, Turkey; ‡Bursa Uludag University School of Medicine, Department of Chest Diseases, Bursa, Turkey.

Originally received Feb. 12, 2021. Final revision May. 29, 2021. Accepted Jun. 28, 2021.

Correspondence to Aysegul Mavi Yildiz, MD, FEBO, FICO, MRCSEd, Bursa Retina Eye Hospital, Bursa, Turkey. dramavi85@hotmail.com